Title: Reducing αENaC expression in the kidney connecting tubule induces pseudohypoaldosteronism type 1 symptoms during K+ loading.

Authors: Poulsen SB, Praetorius J, Damkier HH, Miller L, Nelson RD, Hummler E, Christensen BM

Journal: American journal of physiology. Renal physiology

Year: 2016 Feb 15

Volume: 310

Issue: 4

Pages: F300-10

DOI: 10.1152/ajprenal.00258.2015

Reducing αENaC expression in kidney connecting tubule induces pseudohypoaldosteronism type 1 symptoms during K^+ loading

Søren Brandt Poulsen[1], Jeppe Praetorius[1], Helle H. Damkier[1,2], Lance Miller[3], Raoul D. Nelson[3], Edith Hummler[4] and Birgitte Mønster Christensen[1]

[1]Department of Biomedicine, Aarhus University, Denmark; [2]Department of Cellular and Molecular Medicine, University of Copenhagen, Denmark [3]Department of Pediatrics, University of Utah School of Medicine, United States of America; and [4]Department of Pharmacology and Toxicology, University of Lausanne, Switzerland

Running head: Important role of ENaC in CNT

Correspondence: Birgitte Mønster Christensen, Department of Biomedicine, Aarhus University, Wilhelm Meyers Allé 3, DK-8000 Aarhus C, Denmark (e-mail: bmc@biomed.au.dk; phone: +45 87167629; fax: +45 87167102).

ABSTRACT

Genetic inactivation of the epithelial Na^+ channel α-subunit (αENaC) in the renal collecting duct (CD) does not interfere with Na^+ and K^+ homeostasis in mice. However, inactivation in the CD and a part of the connecting tubule (CNT) induces autosomal recessive pseudohypoaldosteronism type 1 (PHA-1) symptoms already on a standard diet. In the present study, we further examined the importance of αENaC in the CNT. Knock-out mice with αENaC deleted primarily in a part of the CNT (CNT-KO) were generated using *Scnn1a*$^{lox/lox}$ mice and *Atp6v1b1*::*Cre* mice. On a standard diet, plasma [Na^+] and [K^+], and urine Na^+ and K^+ output were unaffected. Seven days of Na^+ restriction (0.01% Na^+) led to a higher urine Na^+ output only on day 3–5, and after 7 days plasma [Na^+] and [K^+] were unaffected. By contrast, the CNT-KO mice were highly susceptible to a 2-day 5% K^+ diet and showed lower food intake and relative body weight, lower plasma [Na^+], higher fractional excretion (FE) of Na^+, higher plasma [K^+], and lower FE of K^+. The higher FE of Na^+ coincided with lower abundance and phosphorylation of the Na^+-Cl^- cotransporter, NCC. In conclusion, reducing ENaC expression in CNT induces clear PHA-1 symptoms during high dietary K^+ loading.

KEYWORDS

αENaC, aldosterone, kidney connecting tubule, sodium, potassium

INTRODUCTION

The functional epithelial Na^+ channel (ENaC) consists of the 3 homologous subunits, α-, β-, and γ (3). Renal ENaC mediates Na^+ reabsorption across the apical plasma membrane of late distal convoluted tubule (DCT2) cells, connecting tubule (CNT) cells, and collecting duct (CD) principal cells (17). Furthermore, ENaC-facilitated K^+ secretion through apical K^+ channels in the CNT and the cortical CD (CCD) may be crucial for maintaining K^+ homeostasis (10). During conditions of hypotension and hyperkalemia, high angiotensin II or K^+ plasma levels stimulate adrenal glomerulosa cells to release the steroid hormone, aldosterone (33). The DCT2/early CNT are largely insensitive to aldosterone, which is in contrast to the late CNT/CCD, where ENaC activity is markedly increased by aldosterone (18, 23).

Loss-of-function mutations in any ENaC subunit may lead to the life-threatening disease, autosomal recessive pseudohypoaldosteronism type 1 (PHA-1). PHA-1 is characterized by, e.g., hyponatremia and hyperkalemia due to impaired ability of the kidney to reabsorb Na^+ and excrete K^+ (4). We have in previous studies generated various αENaC knock-out (KO) mouse lines contributing to an improved understanding of the PHA-1 disease and the physiological importance of the ENaC complex. Global αENaC inactivation is highly critical, leading to neonatal death (12). Inactivation of αENaC in the CD and a part of the CNT (CNT/CD-KO) induces mild hyponatremia on a standard diet and in addition serious weight loss during Na^+ restriction (5). By contrast, CD-specific αENaC KO (CD-KO) mice are unaffected both during Na^+ restriction and high dietary K^+ loading (28). Finally, conditional inactivation of αENaC in the colon (colon-KO) induces fecal Na^+ wasting but this is compensated by the kidney and Na^+ homeostasis is therefore not impaired (19). Hence, these studies collectively point towards a critical role of αENaC particularly in the DCT2 and CNT.

In the present study, we further examined the importance of αENaC in the CNT. KO mice with αENaC deleted primarily in the CNT (CNT-KO) were generated using *Scnn1a*$^{lox/lox}$ mice (13) and *Atp6v1b1*::*Cre* mice. The latter mice have previously been shown to express Cre recombinase in intercalated cells and in approximately 50% of

the CNT cells (20). This correlates with weak V-ATPase B1-subunit expression in some CNT cells (1, 21). We performed a thorough characterization of the *Atp6v1b1*::*Cre* mouse line by crossing it with an enhanced green fluorescent protein (EGFP) reporter mouse line. The CNT-KO mice and the control littermates were examined on standard and challenging diets.

METHODS

Breeding of CNT-KO mice and control littermates, and Cre/EGFP reporter mice

The Cre/loxP recombination system was utilized to investigate the role of ENaC in the CNT for Na^+ and K^+ balance. We used a transgenic mouse line (genetic background: C57BL/6J) in which exon 1 of the gene encoding the α-subunit of ENaC (*Scnn1a*) was flanked by loxP sites [*Scnn1a*$^{lox/lox}$ (13)]. The *Scnn1a*$^{lox/lox}$ mouse line was crossed with a mouse line (genetic background: C57Bl6/CBA) expressing Cre recombinase under the regulatory elements of the *Atp6v1b1* gene (*Atp6v1b1*::*Cre*) encoding the V-ATPase B1-subunit (20). The *Atp6v1b1*::*Cre* mouse line was also recently utilized to inactivate aquaporin-2 genetically in the CNT (16). Interbreeding of *Scnn1a*$^{lox/lox}$ and heterozygous *Atp6v1b1*::*Cre* mice generated *Scnn1a*$^{lox/+}$; *Atp6v1b1*::*Cre* mice, which were further crossed to generate *Scnn1a*$^{lox/lox}$; *Atp6v1b1*::*Cre* mice. Finally, the *Scnn1a*$^{lox/lox}$; *Atp6v1b1*::*Cre* mice were crossed with *Scnn1a*$^{lox/lox}$ mice to generate CNT-KO mice (*Scnn1a*$^{lox/lox}$; *Atp6v1b1*::*Cre*) and control littermates (*Scnn1a*$^{lox/lox}$). The mice were kept on a pelleted mouse chow standard diet (Altromin Spezialfutter GmbH & Co. KG, Lage, Germany) in regular cages at 20°C. Genotyping was carried out by running PCR analyses of tail biopsies using the primers: *Scnn1a* (forward) 5'-CTC AAT CAG AAG GAC CCT GG-3', *Scnn1a* (forward): 5'-GTC ACT GTG TGC ACC CTT AA-3', and *Scnn1a* (reverse): 5'-GCA CAA AGA TCT TAT CCA CC-3', *Cre* (forward): 5'-GTT CGC AAG AAC CTG ATG GAC-3', and *Cre* (reverse)5'-CTA GAG CCT GTT TTG CAC GTT-3' (13).

In order to examine Cre recombinase activity in the *Atp6v1b1*::*Cre* line, these mice were crossed with a dsRed/Cre-inducible EGFP reporter line [B6.Cg-Tg(CAG-DsRed,-EGFP)5Gae/J; The Jackson Laboratory, Bar Harbor, Maine, USA].

Experimental protocols

A mixed population of male and female mice was studied [body weight (BW) CNT-KO mice: 22.9 ± 0.4 g, n = 64; BW control mice: 22.6 ± 0.4 g, n = 60; P = 0.383]. For metabolic experiments, mice were kept in individual metabolic cages (Techniplast, Buguggiate, Italy) at 27°C and initially fed a 3-day specialized standard diet (0.25% Na^+/0.7% K^+; Altromin Spezialfutter GmbH & Co. KG, Lage, Germany). On day 3, baseline parameters were recorded (BW, food intake, water intake, and urine output) after which the mice were put on either a 4-day 0.01% Na^+ diet (age: 10-15 weeks; for immunolabeling only), 7-day 0.01% Na^+ diet (age: 13–28 weeks, two experiments pooled), 4-day 2% K^+ diet (age: 12–25 weeks), or a 2-day 5% K^+ diet (age: 10–37 weeks; two experiments pooled) or a or a 5% K^+/0.01% Na^+ diet (age: 5–25 weeks; two experiments pooled). The diets were given as a mixture of food and water [37.5% water (w/w)]. The added water was included in the total water intake. For experiments in regular cages (blood sampled on standard diet; two experiments were pooled for aldosterone measurements), mice were kept in individual cages at 20°C and fed a pelleted mouse chow diet for 7 days (Altromin Spezialfutter GmbH & Co. KG). Mice had free access to food and water for the duration of all experiments. On the last experimental day, mice were anesthetized by isoflurane inhalation, and blood and tissue were collected. All experimental protocols complied with the European Community guidelines for the use of experimental animals and were performed in agreement with a license issued by the Animal Experiments Inspectorate, Ministry of Food, Agriculture and Fisheries, Danish Veterinary and Food Administration.

Collection and analyses of urine and blood

Urine was collected in metabolic cages and cleared by centrifugation at 1000 *g* for 4 min, and concentrations of Na^+ and K^+ were measured using an IL943™ flame photometer (Instrumentation Laboratory, Bedford, MA, USA; range Na^+ and K^+: 0–200 mM; QC: standards). Blood was collected through the portal vein using a 0.6 x 25 mm needle containing 5 µl Li^+ heparin solution and transferred to heparin-coated centrifuge tubes (PST™ LH Tubes; BD, Franklin Lakes, NJ, USA) and immediately centrifuged at 12,000 *g* for 4 min. Plasma concentrations of Na^+ and K^+ were measured by MRC Harwell (Oxfordshire, UK) and determined using an ion selective electrode (AU680; Beckman Coulter, Brea, CA, USA; range Na^+: 50–200 mM; range K^+: 1.0–10.0 mM, QC: standards). Plasma aldosterone concentrations were determined using an enzyme immunoassay kit (EIA-5298; DRG International Inc., Springfield, NJ, USA; range: 20–1000 pg/ml; QC: standards). Osmolality of urine and plasma was measured using a freezing point depression osmometer (Advanced® Model 3320 Micro-Osmometer; Advanced Instruments, Inc., Norwood, MA, USA; range: 0–2000 mOsm/kg; QC: standards). Urinary NGAL [neutrophil gelatinase-associated lipocalin; a biomarker for acute kidney injury (AKI) (7, 15)] concentrations were measured using a mouse NGAL ELISA kit (Kit 042, Bioporto Diagnostics, Hellerup, Denmark). Samples exceeding the upper limits of the test procedures were diluted according to the manufacturers' protocols.

Immunolabeling

Mice were perfusion fixed via the left ventricle with 3% (v/v) paraformaldehyde in PBS (pH 7.4), where after tissue was post fixed for 1 hour at 4°C. Subsequently, the tissue was gradually dehydrated in ethanol, incubated in xylene, and embedded in paraffin. Using a previously described standard protocol (26), paraffin embedded kidney and colon sections (2 µm) from CNT-KO mice and control mice were labeled with primary αENaC rabbit antibody (28), dilution 1:800). Paraffin-embedded kidney sections from the Cre/EGFP reporter mice were labeled with NCC SPC-402D rabbit

primary antibody (StressMarq Biosciences Inc. Victoria, BC, Canada; dilution 1:200), calbindin (D28K – 10R-C106A) mouse primary antibody (Fitzgerald Industries International, Concord, MA, USA; dilution 1:20.000), AQP2 7661 rabbit primary antibody ((24), dilution 1:1000), and EGFP goat primary antibody (ab6673, Abcam, Cambridge, UK; dilution 1:1000). For light microscopy, immunolabeling was visualized using peroxidase-conjugated goat anti-rabbit secondary antibody (p448; Dako, Glostrup, Denmark; dilution 1:200) and 3,3'-diaminobenzidine (Kem-EN-Tec Diagnostics A/S, Tåstrup, Danmark). For fluorescence microscopy, immunolabeling was visualized using the secondary antibodies (dilution 1:600) donkey anti-goat 488 (Molecular Probes, Life Technologies), donkey anti-rabbit 555 (Molecular Probes, Life Technologies), and donkey anti-mouse 633 (Molecular Probes, Life Technologies).

Microscopy

Counting of αENaC-positive cells in CNT/DCT2 (in cortical labyrinth), and CCD (in medullary arrays) was performed on kidney sections from CNT-KO mice and control mice directly in the microscope (400x magnification). Only cells with a distinct nucleus and apical αENaC labeling were counted. Furthermore, counting was only performed on cells situated in tubules with a clear visible luminal space and with at least one αENaC-positive cell in the tubule. The total number of cells counted in the cortical labyrinth were 345 in the CNT-KO mice (n = 5) and 402 in the control mice (n = 5). The total number of cells counted in medullary arrays were 86 in the CNT-KO mice (n = 5) and 70 in the control mice (n = 5). The fraction of αENaC-positive cells was calculated from the number of αENaC-positive cells divided by the total number of cells counted in each animal. Imaging of kidney and distal colon sections was carried out using a Leica DMRE light microscope equipped with a digital camera (Leica, Wetzlar, Germany). Imaging of kidney and distal colon sections from Cre/EGFP reporter mice (n = 2) were performed using a Leica TCS SL laser scanning confocal microscope and Leica confocal software (Leica). Images were merged using Image J software (Image J, Bethesda, MD, USA). Counting of EGFP-positive cells in the CNT and DCT2 was performed on confocal images taken from Cre/EGFP mice

reporter mice, which were labeled for EGFP, calbindin and NCC (n = 2 animals, one slide from each animal). The images were taken with a 63x objective. The fraction of EGFP-positive CNT cells (strongly calbindin-positive/NCC-negative) was calculated from the number of EGFP-positive/strongly calbindin-positive/NCC-negative cells divided by the total number of strongly calbindin-positive/NCC-negative cells. The fraction of EGFP-positive DCT2 cells (calbindin- and NCC-positive) was calculated from the number of EGFP-positive/calbindin- and NCC-positive cells divided by the total number of calbindin- and NCC-positive cells. The total number of cells counted in the CNT were 132 (n = 2) and 64 in the DCT2 (n = 2).

Semi-quantitative immunoblotting

Tissue was collected, dissected on ice, and immediately homogenized at 4°C in dissection buffer containing protease and phosphatase inhibitors. The homogenates were centrifuged at 1000 *g* for 10 min at 4°C. The supernatants were supplemented with sample buffer to a final concentration of 0.1 M SDS and heated to 65° C for 15 min. Samples were run on Criterion™ TGX™ Precast Gels (4–15% or Any kD; Bio-Rad Laboratories, Hercules, CA, USA) and transferred by electroelution to PVDF membranes (Bio-Rad Laboratories, Hercules, CA, USA) or Hybond-P PVDF membranes (GE Healthcare, Little Chalfont, UK). Subsequently, the membranes were blocked and incubated overnight at 4°C with primary rabbit antibodies [αENaC (30), dilution 1:1000; NKCC2 1495 (9, 14), dilution 1:50; pT96-T101-NKCC2 9934, (6) dilution 1:250]; NCC SPC-402D, dilution 1:1000; pT53-NCC 1246 (25), dilution 1:250; pT58-NCC 1251 (25), dilution 1:1000; or Anti-Kir1.1 (ROMK1) (Alomone, Jerusalem, Israel; dilution 1:400)]. Labeling was visualized using the Enhanced Chemiluminescence system (GE Healthcare, Little Chalfont, UK) or SuperSignal West Femto Chemiluminescent Substrate (Thermo Scientific, Rockford, IL, USA). Because aldosterone might regulate housekeeping genes such as actin, Coomassie-stained gels were used to correct quantification for deviations in protein loading. The maximal deviations in total protein concentration between samples on individual blots were ± 10%.

Statistical analyses

Data meeting statistical assumptions of normality and variance homogeneity were analyzed using Students two-sided *t*-test, while data only meeting assumptions of normality were analyzed using Satterthwaite's two-sided unequal variance *t*-test. Data not meeting assumptions of normality were ln-transformed or square-root transformed in accordance with Sokal and Rohlf (29), and analyzed using the appropriate *t*-tests. If data did not fulfill assumptions of normality after transformation, untransformed data were analyzed using Mann-Whitneys U-test. For parameters where the CNT-KO mice and control mice were compared at multiple time points, *P*-values were adjusted using FDR correction (22). Tests were carried out using Stata 12.0 (StataCorp, College Station, TX, USA) for Windows. All values are presented as mean ± SE.

RESULTS

Evaluation of CNT-KO mice

Breeding of CNT-KO mice and control mice followed Mendelian inheritance (50% *Scnn1a*$^{lox/lox}$; *Atp6v1b1*::*Cre* and 50% *Scnn1a*$^{lox/lox}$, *n* = 204). Using single immunolabeling, counting of αENaC-positive cells in the cortical labyrinth (no discrimination was made between CNT and DCT2) identified αENaC expression in approximately 45% of the cells in the CNT-KO mice, whereas in the control mice the fraction was approximately 70% (Fig. 1*A, B and E*). This corresponded to approximately 40% fewer αENaC-positive cells in the CNT-KO mice ($P < 0.001$). In the CCD (medullary arrays), the CNT-KO mice showed a weak tendency towards fewer αENaC-positive cells (9%; $P = 0.217$; Fig. 1*C, D,* and E). The overall lower fraction of αENaC-positive cells coincided with immunoblotting of cortical/outer medullary (OM) tissue showing 55% lower total protein intensity of αENaC in the CNT-KO mice [both cleaved (30 kD) and full length (90 kD), $P < 0.001$, Fig. 1*F* and *G*]. Cre recombinase activity in the DCT2 was examined by crossing the *Atp6v1b1*::*Cre* mice

with an dsRed/inducible enhanced green fluorescent protein (EGFP) reporter line (Fig. 2 and 3). The progeny expressed EGFP in only a minor portion of the DCT2 cells (approximately 6% [5% and 7%, respectively, in the 2 mice], Fig. 2*A*–*C*), whereas the majority of DCT2 cells were EGFP-negative (Fig. 3*A*–*C*). This indicated that a potential deletion of αENaC in the DCT2 was minimal. Consistent with the lower number of αENaC-positive cells in the CNT-KO, the EGFP reporter mouse expressed EGFP in a high number of the CNT cells (Fig. 2*D*–*I*), while EGFP was absent in the majority of CCD principal cells (Fig. 2*J*–*L* and 3*D*–*F*). Cellular counting revealed that approximately 36% of the CNT cells ([32% and 39%, respectively, in the 2 mice], identified as strongly calbindin-positive and NCC-negative) expressed EGFP. Thus, characterization of the mice indicated that αENaC was inactive primarily in a part of the CNT cells.

Distal colonic αENaC expression was not impaired in the CNT-KO mice.

ENaC is an important mediator of Na^+ reabsorption in the surface epithelial layer of the distal colon (8, 19). It was previously reported that the *Atp6v1b1*::*Cre* mice show unspecific Cre recombinase activity in the colon (20). This could potentially cause inactivation of αENaC in the distal colon of the CNT-KO mice. The Cre/EGFP reporter mice showed no detectable EGFP expression in the surface epithelial layer or in the crypts (Fig. 4*A*). However, some cells in the connective tissue expressed EGFP (Fig. 4*A*, arrows), indicating Cre recombinase activity. We further tested whether αENaC expression was impaired in the distal colon of the CNT-KO mice by using immunolabeling and immunoblotting. Immunolabeling detected αENaC in the surface epithelial layer of both CNT-KO mice and control mice kept on a 4-day 0.01% Na^+ diet (Fig. 4*B* and *C*). Immunoblotting demonstrated that the abundance of total αENaC [(cleaved (30 kD) + full length (90 kD)] did not differ between CNT-KO mice and control mice kept on the 7-day 0.01% Na^+ diet [$P = 0.512$; Fig.4 and *E*]. However, the 30 kD/90 kD ratio was higher in the CNT KO mice [$P = 0.017$, Fig. 4*D* and *E*], suggesting greater cleavage of αENaC and thus, increased activity [reviewed in (27)]. A non-regulated band was found at 55 kD [CNT-KO mice: 1.00 ± 0.08 ($n = 9$), control

mice: 1.00 ± 0.22 (n = 9), P = 0.986, Fig. 4*D* and *E*], but whether this was a cleaved form of αENaC was not further examined. Collectively, data demonstrated that αENaC expression was not impaired in the distal colon of the CNT-KO mice.

Phenotyping of CNT-KO mice on standard and challenging diets.

To examine the effect of genetic αENaC inactivation in the CNT on Na^+ and K^+ homeostasis, CNT-KO mice and control mice were examined on a standard diet (baseline), 7-day 0.01% Na^+ diet, 4-day 2% K^+ diet, a 2-day 5% K^+ diet, or a 5% K^+/0.01% Na^+ diet.

Standard diet. When fed a standard diet in regular cages, no differences were found in plasma [Na^+], [K^+], creatinine concentration, or osmolality between CNT-KO mice and control mice (Fig. 5*A*, *B*, *D* and *E*). However, the plasma aldosterone concentration was higher in the CNT-KO mice (P < 0.01, Fig. 5*C*). Baseline measurements in metabolic cages did not show any differences in the tested parameters [relative body weight (BW), food intake, water intake, urine output, urine Na^+ and K^+ output, and urine osmolality; Fig. 6*A*–*U*]. Similarly, no significant differences in these parameters were observed when pooling baseline data (collected over the last 24 h prior to diet manipulation) from the metabolic cage experiments (data not shown).

Seven-day 0.01% Na^+ diet. Challenging the CNT-KO mice with a 7-day 0.01% Na^+ diet did not affect plasma [Na^+], [K^+], creatinine concentration, or osmolality (Fig. 5*A*, *B*, *D* and *E*), however, the plasma aldosterone concentration was still higher compared to the control mice (P < 0.01, day 7, Fig. 5*C*). On day 3–5, the CNT-KO mice excreted more Na^+ in the urine than the control mice (P between 0.01 and 0.05; Fig. 6*E*), however, the difference diminished on day 6 and eventually disappeared on day 7 [not significant (NS), Fig. 6*E*]. The urine osmolality was higher in the CNT-KO mice on day 4 and 7 (P < 0.05, Fig. 6*G*) compared to the control mice, whereas no differences were found in relative BW, food intake, water intake, urine output, and urine K^+ excretion (Fig. 6*A*–*D* and *F*).

Four-day 2% K^+ diet. When challenged with a 4-day 2% K^+ diet, plasma [Na^+], [K^+], creatinine concentration, and osmolality (Fig. 5*A*, *B*, and *D*) did not differ between the CNT-KO mice and the control mice, however, the plasma aldosterone concentration was clearly higher (day 4: $P < 0.001$, Fig. 5*C*). By contrast, no differences were found in relative BW, food and water intake, urine output, urine Na^+ and K^+ output, and urine osmolality (Fig. 6*H*–*N*).

Two-day 5% K^+ diet. The 2-day 5% K^+ diet induced a lower relative BW in the CNT-KO mice compared to the control mice (day 1: $P < 0.001$; day 2: $P < 0.001$; Fig. 6*O*), which was accompanied by lower plasma [Na^+] (day 2: $P < 0.001$, Fig. 5*A*). The total urine Na^+ output was unaffected (NS, Fig. 6*S*), however, the CNT-KO mice consumed less food (and thereby less Na^+) than the control mice (day 1: $P < 0.001$; day 2: $P < 0.01$; Fig. 6*P*). This was taken into account by calculating the Na^+ output (urine)/intake (food) ratio. The Na^+ output/intake ratio was higher in the CNT-KO mice compared to the control mice on both day 1 ($P < 0.001$, Table 1) and day 2 ($P < 0.01$, Table 1). Furthermore, the fractional excretion (FE) of Na^+ was higher in the CNT-KO mice when measured on day 2 ($P < 0.01$, Table 1). In terms of K^+ homeostasis, the CNT-KO mice presented higher plasma [K^+] (day 2: $P < 0.001$, Fig. 5*B*) and lower urine K^+ output (day 1: $P < 0.001$, day 2: $P < 0.05$, Fig. 6*T*) compared to the control mice, but the K^+ output/intake ratio was not different, neither on day 1 nor day 2 (NS, Table 1). However, the FE of K^+ was lower in CNT-KO mice when measured on day 2 ($P < 0.05$, Table 1), indicating impaired K^+ excretion. Finally, the CNT-KO mice showed higher plasma aldosterone concentration (day 2: $P < 0.001$, Fig. 5*C*), creatinine concentration ($P < 0.01$, Table 1), and lower glomerular filtration rate (GFR; $P < 0.05$, Table 1), water intake (day 1: $P < 0.01$, Fig. 6*Q*), and urine output (day 1: $P < 0.05$, Fig. 6*R*) than the control mice. NGAL concentrations were measured in urine samples collected on day 2. There were no significant differences in urinary NGAL concentrations [CNT-KO mice: 150.8 ± 52.4 ng/ml ($n = 10$), control mice: 85.8 ± 35.4 ng/ml ($n = 8$), $P = 0.131$] or in urinary NGAL excretion [CNT-KO mice: 32.0 ± 11.6 ng/g BW/24 h ($n = 10$), control mice: 16.6 ± 6.8 ng/g BW/24 h ($n = 8$), $P = 0.248$].

Mice were, furthermore, tested on a 2-day 5% K^+/0.01% Na^+ diet. The control mice showed lower relative BW both on day 1 ($P < 0.001$) and day 2 ($P < 0.001$) compared to baseline, suggesting that BW loss during K^+ loading was not specific for the CNT-KO mice, but could be induced in control mice when combining K^+ loading and Na^+ restriction. However, the weight loss was less severe in the control mice compared to the CNT-KO both on day 1 (control: 0.96 ± 0.01, $n = 10$; KO: 0.91 ± 0.00, $n = 10$; $P < 0.001$) and day 2 (control: 0.94 ± 0.01, $n = 10$; KO: 0.86 ± 0.01, $n = 10$; $P < 0.001$).

The CNT-KO mice presented lower abundance and phosphorylation of NCC on a 5% K^+ diet

Hyperkalemia is connected with reduced Na^+ reabsorption in the thick ascending limb (TAL) and the distal convoluted tubule (DCT), leading to increased Na^+ delivery to ENaC-expressing tubular segments thereby favoring K^+ secretion (30, 31, 34, 35). Therefore, we tested whether the higher FE of Na^+ in the CNT-KO mice compared to the control mice during K^+ loading occurred in parallel with lower protein abundance and phosphorylation of the Na^+-K^+-$2Cl^-$ cotransporter, NKCC2 (expressed in TAL), and the Na^+-Cl^- cotransporter, NCC (expressed in DCT). Immunoblotting of cortical/OM tissue (collected on day 2) showed no differences in the protein abundances of NKCC2, pT96-T101-NKCC2, or the pT96-T101-NKCC2/NKCC2 ratio (NS, Fig. 7). By contrast, we found a lower abundance of total NCC ($P < 0.05$, Fig. 7), pT53-NCC ($P < 0.01$, Fig. 7), and pT58-NCC ($P < 0.001$, Fig. 7). Furthermore, the pT53-NCC/NCC ($P < 0.05$, Fig. 7) and the pT58-NCC/NCC ratios ($P < 0.001$, Fig. 7) were lower in the CNT-KO mice, suggesting that the lower phosphorylation of NCC was not a result of lower total NCC protein abundance *per se*. Finally, no effect was found on ROMK abundance (Fig. 7). Collectively, the higher FE of Na^+ in the CNT-KO mice fed a 5% K^+ diet coincided with lower abundance and phosphorylation of NCC in the DCT and lower αENaC expression in the CNT.

DISCUSSION

This study provides novel insight into the physiological role of αENaC in the kidney and the activation of compensatory mechanisms in a conditional model of the PHA-1 syndrome. CNT-KO mice showed a severe phenotype when examined on a 5% K^+ diet as evidenced by e.g. higher plasma [K^+] and lower FE of K^+. This could be a result of impaired ENaC-mediated K^+ secretion in CNT through apical K^+ channels such as ROMK (2). Although the CNT-KO mice were unable to maintain K^+ balance to the same extent as the controls, data indicated that compensatory mechanisms did take place. The mice presented higher plasma aldosterone level and lower abundance and phosphorylation of the DCT-specific Na^+ transporter, NCC, indicating lower Na^+ reabsorption in the DCT. Inhibition of Na^+ reabsorption in the TAL and the DCT during hyperkalemia may lead to higher tubular flow rate and Na^+ delivery to ENaC-expressing tubule segments (30, 31, 34, 35), producing a favorable gradient for K^+ secretion in the CNT and CCD. Thus, a compensatory target in our model could be NCC in the DCT. By contrast, we did not observe a significantly lower abundance or phosphorylation of NKCC2, which is vital for Na^+ reabsorption in the TAL and macula densa. Another potential compensatory target is ROMK, but our data did not show any changes in ROMK abundance either.

On the 5% K^+ diet, lower NCC activity, together with inactivation of αENaC in the CNT, coincided with higher FE of Na^+ and Na^+ output/intake ratio in the CNT-KO mice. Importantly, this suggests that in the CNT-KO mice, ENaC in the CD was not sufficient to effectively reabsorb a higher Na^+ delivery. Collectively, these events may have induced the lower plasma [Na^+] in the CNT-KO mice. To exclude that the phenotype could be a result of AKI, urinary NGAL concentrations were determined on day 2. The lack of differences in both urinary NGAL concentration and excretion as well as the lack of differences in urine output and water intake between the CNT-KO mice and the control mice on day 2 indicated that the CNT-KO mice had not developed AKI. We did not observe any difference in total urinary Na^+ output after 1 and 2 days of 5% K^+ loading, however, it cannot be excluded that a potential difference in Na^+ output could be detected at earlier time points (i.e. after minutes) (30).

406 The CNT-KO mice presented higher aldosterone levels on the low-Na^+ diet and a
407 mild phenotype as evidenced by Na^+ wasting on day 3–5. However, this effect
408 eventually disappeared after 7 days, after which no effects were found on plasma
409 [Na^+] and [K^+]. Data indicated higher cleavage of ENaC in the distal colon and this
410 potential activation of ENaC could, at least partially, have compensated for reduced
411 renal Na^+ reabsorption in the CNT.
412 We have previously shown that genetic inactivation of αENaC in the CD did not
413 interfere with Na^+ and K^+ balance in mice kept on a standard diet, low-Na^+ diet, or a
414 6% K^+ diet (28). This suggests that αENaC in the CD is apparently not a prerequisite
415 for maintaining Na^+ and K^+ homeostasis. By contrast, combined αENaC inactivation in
416 a part of the CNT (approximately 30% fewer αENaC-positive cells in early CNT, and
417 70% fewer αENaC-positive cells in late CNT) and CD induced PHA-1 symptoms
418 already on a standard diet as evidenced by natriuresis, hyponatremia, and
419 hyperkalemia (5). During Na^+ restriction, the CNT/CD-KO mice showed lower relative
420 BW, severe urine Na^+ loss, hyponatremia, and hyperkalemia (5). Thus, the phenotype
421 was stronger in the CNT/CD-KO mice than in the CNT-KO mice on a standard diet or a
422 low-Na^+ diet. Besides a potential compensation in the colon, it is possible that the CD
423 in the CNT-KO mice could partially compensate for the lack of αENaC in the CNT.
424 Because αENaC was deleted in the CD of the CNT/CD-KO mice, such compensation
425 was not possible in these mice. However, it cannot be ruled out either that the
426 deletion of αENaC in the CNT-KO was less efficient than in the CNT/CD-KO mice
427 thereby explaining the milder phenotype. Thus, it is possible that the remaining CNT
428 cells still expressing αENaC in the CNT-KO were sufficient to maintain proper Na^+
429 balance.
430 A 5% K^+ diet induced a weaker phenotype in the CNT/CD-KO mice than in the
431 CNT-KO mice. Both mouse lines showed lower plasma [Na^+] and higher plasma [K^+]
432 on the 5% K^+ diet, however, the CNT-KO mice additionally presented lower food
433 intake and lower relative BW, whereas these parameters were unaffected in the
434 CNT/CD-KO mice. Impaired ENaC-facilitated K^+ secretion in the colon (11, 32), was
435 not likely to cause the stronger phenotype in the CNT-KO mice, because the colonic
436 αENaC expression was intact. Although the role of ENaC in the DCT2 for K^+ secretion

is unknown, it could be speculated that deletion of αENaC only in a few DCT2 cells could become critical during K^+ loading.

In summary, we examined the importance of αENaC in the CNT by generating KO mice in which αENaC was deleted primarily in the CNT. The mice showed no obvious phenotype on a standard diet, 0.01% Na^+ diet, or a 2% K^+ diet. The elevated aldosterone levels in the CNT-KO mice may stimulate ENaC activity in the late CNT (in remaining ENaC expressing cells), in the CD, or in the colon and potentially compensate for the reduced Na^+ reabsorption in the CNT. On a 5% K^+ diet, however, the mice presented clear PHA-1 symptoms. Our data provide an unprecedented insight into compensatory mechanisms taking place in a conditional model of the PHA-1 syndrome. Even when αENaC is deleted only in a part of the CNT, several compensatory mechanisms occur. During 5% K^+ loading, this includes higher plasma aldosterone level, lower renal NCC activity, and lower GFR. Clinically, the results may contribute to a deeper understanding of how the body copes with the physiological challenges that are taking place in PHA-1 patients.

ACKNOWLEDGMENTS

The antibodies against αENaC, and pT53-NCC and pT58-NCC used for semi-quantitative immunoblotting were kindly provided by J. Loffing (Institute of Anatomy, University of Zurich, Switzerland) and R. Fenton (Department of Biomedicine, Aarhus University, Denmark), respectively. We thank J. Frøkiær (Department of Clinical Medicine, Aarhus University Hospital, Aarhus, Denmark) for help on measuring urine [Na^+] and [K^+], and I. M. S. Paulsen, H. Høyer, C. Westberg, T. Drejer, P. A. Nielsen, and M. S. Gandry for technical assistance.

GRANTS

Funding for this study was provided by the Danish Council for Independent Research (B.M.C.), the Lundbeck Foundation (B.M.C.), the Danish Heart Foundation (B.M.C.), and Health (Faculty of Health Sciences, Aarhus University; S.B.P.).

DISCLOSURES

None.

AUTHOR CONTRIBUTIONS

S.B.P.: conception and design of the experiments; collection, analysis, and interpretation of data; drafting the article or revising it critically for important intellectual content; J.P.: drafting the article or revising it critically for important intellectual content; H.H.D.: collection of data; drafting the article or revising it critically for important intellectual content; L.M.: drafting the article or revising it critically for important intellectual content; R.D.N.: drafting the article or revising it critically for important intellectual content; E.H.: drafting the article or revising it critically for important intellectual content; B.M.C.: conception and design of the experiments; collection, analysis, and interpretation of data; drafting the article or revising it critically for important intellectual content; All authors approved the final version of the manuscript.

REFERENCES

1. **Alper SL, Natale J, Gluck S, Lodish HF and Brown D**. Subtypes of intercalated cells in rat kidney collecting duct defined by antibodies against erythroid band 3 and renal vacuolar H^+-ATPase. *Proc Natl Acad Sci U S A* 86: 5429-5433, 1989.

2. **Arroyo JP, Ronzaud C, Lagnaz D, Staub O and Gamba G**. Aldosterone paradox: differential regulation of ion transport in distal nephron. *Physiology (Bethesda)* 26: 115-123, 2011.

3. **Canessa CM**. Structural biology: unexpected opening. *Nature* 449: 293-294, 2007.

4. **Chang SS, Grunder S, Hanukoglu A, Rosler A, Mathew PM, Hanukoglu I, Schild L, Lu Y, Shimkets RA, Nelson-Williams C, Rossier BC and Lifton RP**. Mutations in subunits of the epithelial sodium channel cause salt wasting with hyperkalaemic acidosis, pseudohypoaldosteronism type 1. *Nat Genet* 12: 248-253, 1996.

5. **Christensen BM, Perrier R, Wang Q, Zuber AM, Maillard M, Mordasini D, Malsure S, Ronzaud C, Stehle JC, Rossier BC and Hummler E**. Sodium and potassium balance depends on alphaENaC expression in connecting tubule. *J Am Soc Nephrol* 21: 1942-1951, 2010.

6. **Dimke H, Flyvbjerg A, Bourgeois S, Thomsen K, Frokiaer J, Houillier P, Nielsen S and Frische S**. Acute growth hormone administration induces antidiuretic and antinatriuretic effects and increases phosphorylation of NKCC2. *Am J Physiol Renal Physiol* 292: F723-F735, 2007.

7. **Doi K, Katagiri D, Negishi K, Hasegawa S, Hamasaki Y, Fujita T, Matsubara T, Ishii T, Yahagi N, Sugaya T and Noiri E**. Mild elevation of urinary biomarkers in prerenal acute kidney injury. *Kidney Int* 82: 1114-1120, 2012.

8. **Duc C, Farman N, Canessa CM, Bonvalet JP and Rossier BC**. Cell-specific expression of epithelial sodium channel alpha, beta, and gamma subunits in aldosterone-responsive epithelia from the rat: localization by in situ hybridization and immunocytochemistry. *J Cell Biol* 127: 1907-1921, 1994.

9. **Ecelbarger CA, Terris J, Hoyer JR, Nielsen S, Wade JB and Knepper MA**. Localization and regulation of the rat renal Na(+)-K(+)-2Cl- cotransporter, BSC-1. *Am J Physiol* 271: F619-F628, 1996.

10. **Giebisch G**. Renal potassium transport: mechanisms and regulation. *Am J Physiol* 274: F817-F833, 1998.

11. **Grotjohann I, Gitter AH, Kockerling A, Bertog M, Schulzke JD and Fromm M**. Localization of cAMP- and aldosterone-induced K^+ secretion in rat distal colon by conductance scanning. *J Physiol* 507: 561-570, 1998.

12. **Hummler E, Barker P, Gatzy J, Beermann F, Verdumo C, Schmidt A, Boucher R and Rossier BC**. Early death due to defective neonatal lung liquid clearance in alpha-ENaC-deficient mice. *Nat Genet* 12: 325-328, 1996.

13. **Hummler E, Merillat AM, Rubera I, Rossier BC and Beermann F**. Conditional gene targeting of the Scnn1a (alphaENaC) gene locus. *Genesis* 32: 169-172, 2002.

14. **Jensen AM, Norregaard R, Topcu SO, Frokiaer J and Pedersen M**. Oxygen tension correlates with regional blood flow in obstructed rat kidney. *J Exp Biol* 212: 3156-3163, 2009.

15. **Kawano H, Muto S, Ohmoto Y, Iwata F, Fujiki H, Mori T, Yan L and Horie S**. Exploring urinary biomarkers in autosomal dominant polycystic kidney disease. *Clin Exp Nephrol* 2014.

16. **Kortenoeven ML, Pedersen NB, Miller RL, Rojek A and Fenton RA**. Genetic ablation of aquaporin-2 in the mouse connecting tubules results in defective renal water handling. *J Physiol* 591: 2205-2219, 2013.

17. **Loffing J and Kaissling B**. Sodium and calcium transport pathways along the mammalian distal nephron: from rabbit to human. *Am J Physiol Renal Physiol* 284: F628-F643, 2003.

18. **Loffing J, Zecevic M, Feraille E, Kaissling B, Asher C, Rossier BC, Firestone GL, Pearce D and Verrey F**. Aldosterone induces rapid apical translocation of ENaC in early portion of renal collecting system: possible role of SGK. *Am J Physiol Renal Physiol* 280: F675-F682, 2001.

19. **Malsure S, Wang Q, Charles RP, Sergi C, Perrier R, Christensen BM, Maillard M, Rossier BC and Hummler E**. Colon-specific deletion of epithelial sodium channel causes sodium loss and aldosterone resistance. *J Am Soc Nephrol* 25: 1453-1464, 2014.

20. **Miller RL, Lucero OM, Riemondy KA, Baumgartner BK, Brown D, Breton S and Nelson RD**. The V-ATPase B1-subunit promoter drives expression of Cre recombinase in intercalated cells of the kidney. *Kidney Int* 75: 435-439, 2009.

21. **Miller RL, Zhang P, Smith M, Beaulieu V, Paunescu TG, Brown D, Breton S and Nelson RD**. V-ATPase B1-subunit promoter drives expression of EGFP in intercalated cells of kidney, clear cells of epididymis and airway cells of lung in transgenic mice. *Am J Physiol Cell Physiol* 288: C1134-C1144, 2005.

22. **Narum SR**. Beyond Bonferroni: less conservative analyses for conservation genetics. *Conserv Genet* 7: 783-787, 2006.

23. **Nesterov V, Dahlmann A, Krueger B, Bertog M, Loffing J and Korbmacher C**. Aldosterone-dependent and -independent regulation of the epithelial

562 sodium channel (ENaC) in mouse distal nephron. *Am J Physiol Renal Physiol*
563 303: F1289-F1299, 2012.

564 24. **Nielsen J, Kwon TH, Praetorius J, Frokiaer J, Knepper MA and Nielsen S**.
565 Aldosterone increases urine production and decreases apical AQP2 expression
566 in rats with diabetes insipidus. *Am J Physiol Renal Physiol* 290: F438-F449,
567 2006.

568 25. **Pedersen NB, Hofmeister MV, Rosenbaek LL, Nielsen J and Fenton RA**.
569 Vasopressin induces phosphorylation of the thiazide-sensitive sodium
570 chloride cotransporter in the distal convoluted tubule. *Kidney Int* 78: 160-169,
571 2010.

572 26. **Poulsen SB, Kim YH, Frokiaer J, Nielsen S and Christensen BM**. Long-term
573 vasopressin-V2-receptor stimulation induces regulation of aquaporin 4
574 protein in renal inner medulla and cortex of Brattleboro rats. *Nephrol Dial*
575 *Transplant* 28: 2058-2065, 2013.

576 27. **Rossier BC and Stutts MJ**. Activation of the epithelial sodium channel (ENaC)
577 by serine proteases. *Annu Rev Physiol* 71: 361-379, 2009.

578 28. **Rubera I, Loffing J, Palmer LG, Frindt G, Fowler-Jaeger N, Sauter D, Carroll**
579 **T, McMahon A, Hummler E and Rossier BC**. Collecting duct-specific gene

580 inactivation of alphaENaC in the mouse kidney does not impair sodium and
581 potassium balance. *J Clin Invest* 112: 554-565, 2003.

582 29. **Sokal RR and Rohlf FJ**. In: Biometry, edited by W.H.Freeman and Company.
583 New York: 1995.

584 30. **Sorensen MV, Grossmann S, Roesinger M, Gresko N, Todkar AP,**
585 **Barmettler G, Ziegler U, Odermatt A, Loffing-Cueni D and Loffing J**. Rapid
586 dephosphorylation of the renal sodium chloride cotransporter in response to
587 oral potassium intake in mice. *Kidney Int* 83: 811-824, 2013.

588 31. **Stokes JB**. Consequences of potassium recycling in the renal medulla. Effects
589 of ion transport by the medullary thick ascending limb of Henle's loop. *J Clin*
590 *Invest* 70: 219-229, 1982.

591 32. **Sweiry JH and Binder HJ**. Characterization of aldosterone-induced potassium
592 secretion in rat distal colon. *J Clin Invest* 83: 844-851, 1989.

593 33. **Thomas W and Harvey BJ**. Mechanisms underlying rapid aldosterone effects
594 in the kidney. *Annu Rev Physiol* 73: 335-357, 2011.

595 34. **Vallon V, Schroth J, Lang F, Kuhl D and Uchida S**. Expression and
596 phosphorylation of the Na^+-Cl^- cotransporter NCC in vivo is regulated by

597 dietary salt, potassium, and SGK1. *Am J Physiol Renal Physiol* 297: F704-F712,
598 2009.

599 35. **van der Lubbe N, Moes AD, Rosenbaek LL, Schoep S, Meima ME, Danser**
600 **AH, Fenton RA, Zietse R and Hoorn EJ**. K^+-induced natriuresis is preserved
601 during Na^+ depletion and accompanied by inhibition of the Na^+-Cl^-
602 cotransporter. *Am J Physiol Renal Physiol* 305: F1177-F1188, 2013.

603 **FIGURE LEGENDS**

604

605 Fig. 1. αENaC expression was lower in the CNT-KO mice. *A*–*D*, in mice kept on a 4-day
606 0.01% Na^+ diet, immunolabeling showed more αENaC-positive cells in the CNT/DCT2
607 (in the cortical labyrinth) of controls (*A*, arrows indicate αENaC-positive cells) than in
608 the CNT-KO mice (*B*, arrow heads indicate αENaC-negative cells). *E*, the fraction of
609 αENaC-positive cells in the CNT/DCT2 was approximately 40% lower in the CNT-KO
610 mice, whereas no significant difference was found in the CCD (C–E, arrows indicate
611 αENaC-positive cells, in medullary arrays). *F* and *G*, on a standard diet, the CNT-KO
612 mice showed 55% lower total αENaC protein intensity in cortical/outer medullary
613 tissue homogenate [cleaved (30 kD) + full length (90 kD)]. Each bar indicates mean ±
614 SE. $^{**}P < 0.01$, $^{***}P < 0.001$.

615

616 Fig. 2. *Atp6v1b1*::*Cre*/enhanced green fluorescent protein (EGFP) reporter mice
617 expressed EGFP in AQP2 and calbindin-positive cells in the CNT, whereas only a few
618 NCC-positive cells in the DCT2 and a few AQP2-positive cells in the CCD were EGFP
619 positive. Calbindin was used a marker for CNT/DCT2. A–C, arrow: NCC-
620 positive/EGFP-positive cell. D–F, arrow: calbindin-positive/EGFP-positive cell;
621 arrowhead: calbindin-negative/EGFP-positive cell; asterisk: calbindin-positive/EGFP-
622 negative cell. G–I, arrow: calbindin-positive/AQP2-positive/EGFP-positive cell;
623 arrowhead: AQP2-negative/EGFP-positive cell. J–L, arrow: AQP2-positive/EGFP-
624 positive cell; arrowhead: AQP2-negative/EGFP-positive cell; asterisk: AQP2-
625 positive/EGFP-negative cell. Glo: glomerulus.

626 Fig. 3. The majority of NCC-positive cells in the DCT2 and AQP2-positive cells in the
627 CCD did not express EGFP in the *Atp6v1b1*::*Cre*/EGFP reporter mice. A–C, arrowhead:
628 NCC-negative/EGFP-positive cell; asterisks: NCC-positive/EGFP-negative cells. D–F,
629 arrowhead: AQP2-negative/EGFP-positive cell; asterisks: AQP2-positive/EGFP-
630 negative cells.

631

Fig. 4. Distal colonic αENaC expression was not impaired in the CNT-KO mice. *A*, *Atp6v1b1*::*Cre*/EGFP reporter mice showed EGFP expression in some cells of the connective tissue in the distal colon (arrows), whereas EGFP was not detectable in the surface epithelial layer (n = 2). *B*, in the control mice and *C*, the CNT-KO mice kept on a 4-day 0.01% Na^+ diet, immunolabeling revealed clear apical labelling in the distal colonic surface epithelial layer. *D* and *E*, immunoblotting and corresponding densitometric analyses of distal colonic homogenates showed that total αENaC abundance (30+90 kD bands, arrows) did not differ between the control mice and the CNT-KO mice kept on a 7-day 0.01% Na^+ diet. The 30/90 kD-ratio was, however, higher in the CNT-KO mice than in the control mice. Each bar indicates mean ± SE. *P < 0.05. LU: lumen, CR: crypt.

Fig. 5. Blood parameters: the CNT-KO mice presented a clear phenotype on a 5% K^+ diet. Effects of various diets on, *A*, plasma [Na^+], *B*, plasma [K^+], *C*, plasma aldosterone concentration, *D*, plasma creatinine concentration, and, *E*, plasma osmolality in the control mice and the CNT-KO mice. The mice were kept on either a standard diet in regular cages ([Na^+], [K^+], creatinine and osmolality: control n = 7, KO n = 9; aldosterone: control n = 14, KO n = 17), 7-day 0.01% Na^+ diet in metabolic cages ([Na^+], [K^+], aldosterone, and osmolality: control n = 17, KO n = 18; creatinine: control n = 15, KO n = 15), 4-day 2% K^+ diet in metabolic cages (control n = 9, KO n = 9), or a 2-day 5% K^+ diet in metabolic cages (control n = 8, KO n = 10). Each bar indicates mean ± SE. **P < 0.01, ***P < 0.001.

Fig. 6. Metabolic parameters: the CNT-KO mice presented a clear phenotype on a 5% K^+ diet. The control mice and the CNT-KO mice were kept in metabolic cages on a standard diet (baseline) followed by either a, *A*–*G*, 7-day 0.01% Na^+ diet (control n = 17–18, KO n = 17–18), *H*–*N*, 4-day 2% K^+ diet (control n = 9, KO n = 9), or, *O*–*U*, a 2-day 5% K^+ diet (*O*–*R*, control n = 17, KO n = 18; *S*–*U*, control n = 9, KO n = 8). Each circle indicates mean ± SE. *P < 0.05, **P < 0.01, ***P < 0.001.

662 Fig. 7. The CNT-KO mice presented lower abundance and phosphorylation of NCC on
663 a 5% K^+ diet. Presented are protein abundances of NKCC2, p-NKCC2 (pT96/T101),
664 NCC, pT53-NCC, pT58-NCC, and ROMK in control mice (n = 8) and CNT-KO mice (n =
665 10) as determined by immunoblotting of cortical/outer medullary tissue
666 homogenates. Furthermore, presented are the ratios of pT96-T101-NKCC2/NKCC2,
667 pT53-NCC/NCC, and pT58-NCC/NCC. Each bar indicates mean ± SE. *P < 0.05, **P <
668 0.01, ***P < 0.001.

669

TABLES

Table 1. Urine and plasma parameters in control mice and CNT-KO mice kept on a 2-day 5% K^+ diet

Parameter		Control			KO			*P*
		Mean	SE	*n*	Mean	SE	*n*	
Na^+ output/intake ratio	Baseline	0.73	0.07	9	0.71	0.06	8	NS
	day 1	0.98	0.05	9	1.47	0.07	8	< 0.001
	day 2	0.72	0.04	9	0.95	0.05	8	< 0.01
K^+ output/intake ratio	Baseline	0.72	0.05	9	0.66	0.06	8	NS
	day 1	0.73	0.03	9	0.60	0.04	8	NS
	day 2	0.69	0.03	9	0.70	0.04	8	NS
FE Na^+ (%)	day 2	0.42	0.03	8	0.56	0.03	10	< 0.01
FE K^+ (%)	day 2	71	7	8	51	5	10	< 0.05
Plasma creatinine (mM)	day 2	7.6	0.4	8	11.0	0.7	10	< 0.01
GFR (µl/min)	day 2	290	30	8	219	17	10	< 0.05

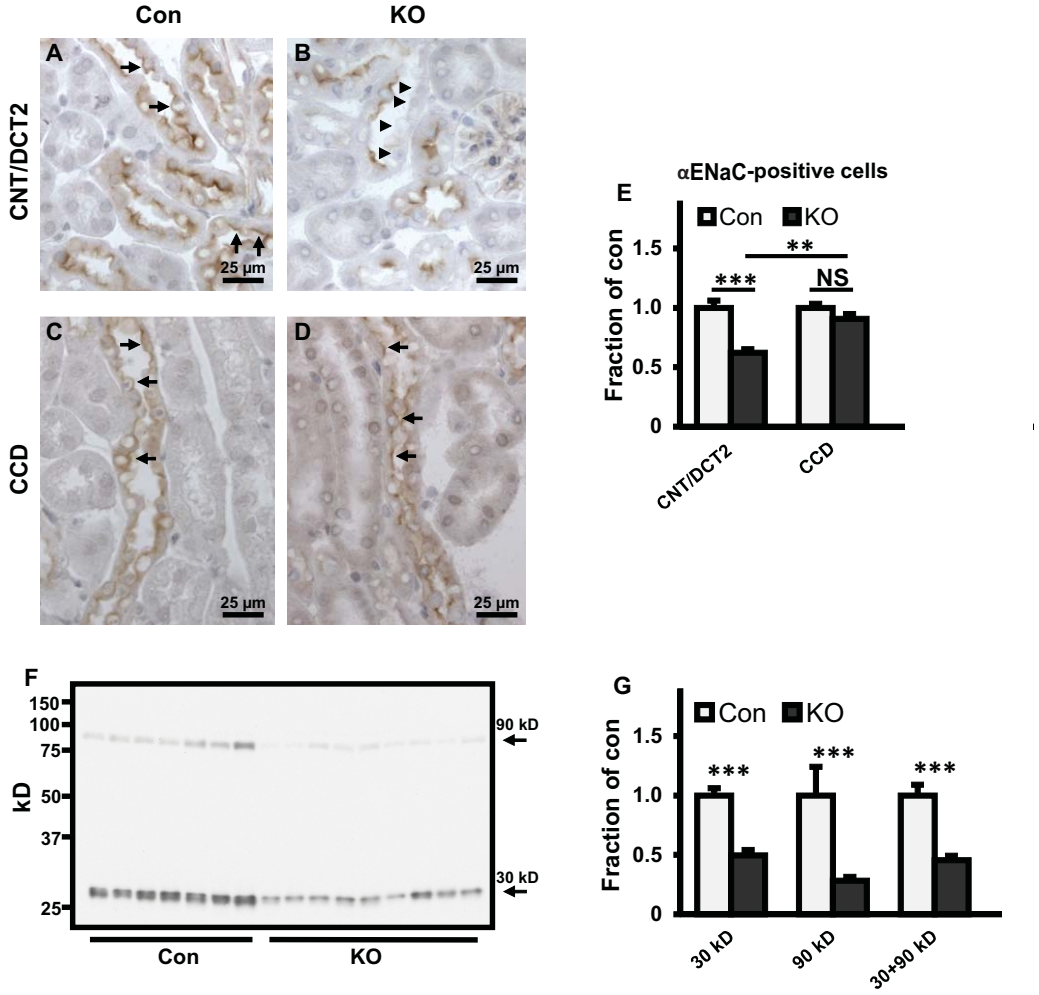
Con
KO
A
B
C
D
CNT/DCT2
CCD
25 μm
αENaC-positive cells
E
Con
KO
Fraction of con
1.5
1.0
0.5
0
***
**
NS
CNT/DCT2
CCD
F
150
100
75
50
37
25
kD
90 kD
30 kD
Con
KO
G
Con
KO
Fraction of con
1.5
1.0
0.5
0
***
***
***
30 kD
90 kD
30+90 kD

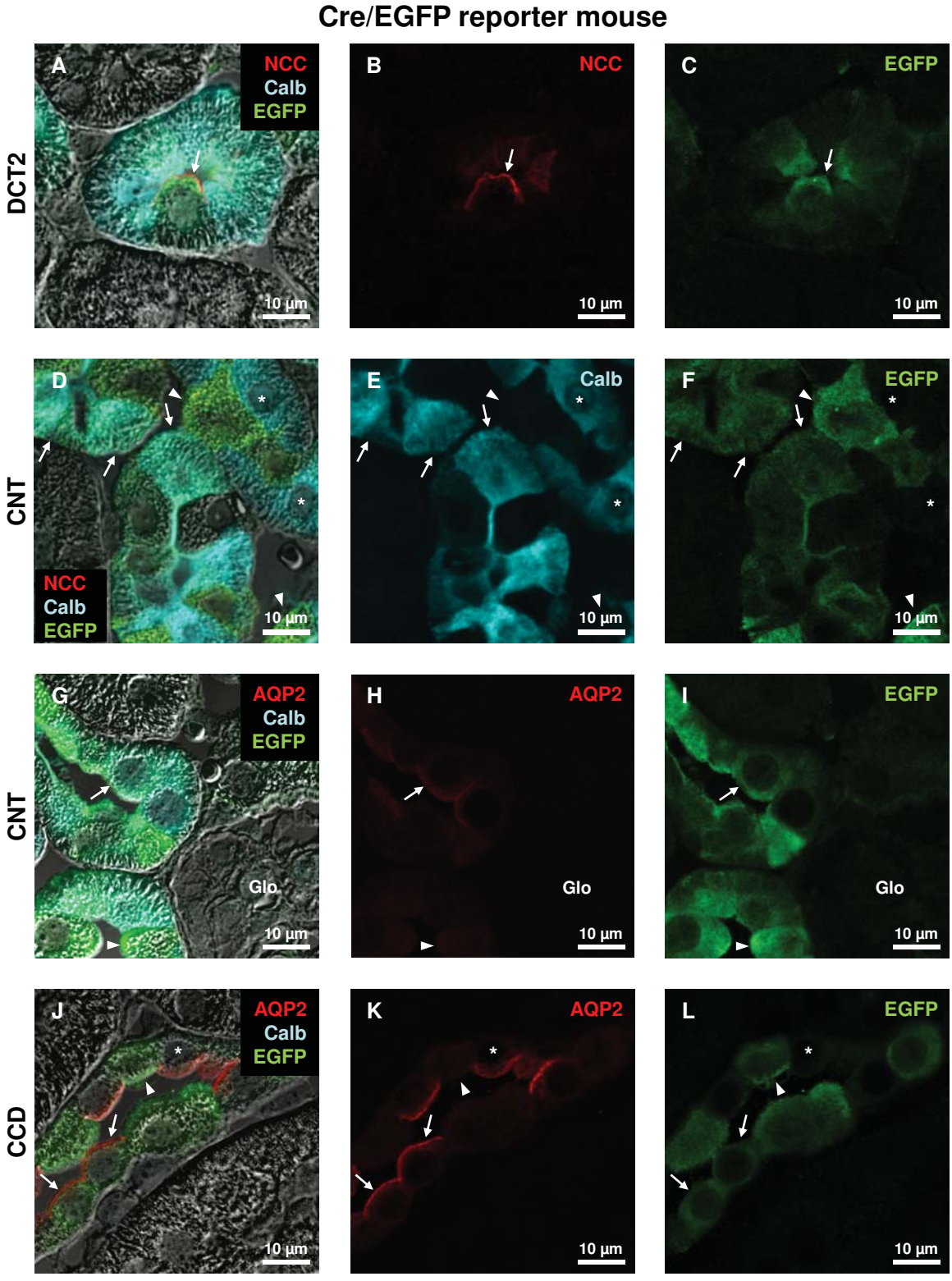
Cre/EGFP reporter mouse
DCT2
CNT
CNT
CCD
A
NCC
Calb
EGFP
10 µm
B
NCC
10 µm
C
EGFP
10 µm
D
NCC
Calb
EGFP
10 µm
E
Calb
10 µm
F
EGFP
10 µm
G
AQP2
Calb
EGFP
Glo
10 µm
H
AQP2
Glo
10 µm
I
EGFP
Glo
10 µm
J
AQP2
Calb
EGFP
10 µm
K
AQP2
10 µm
L
EGFP
10 µm

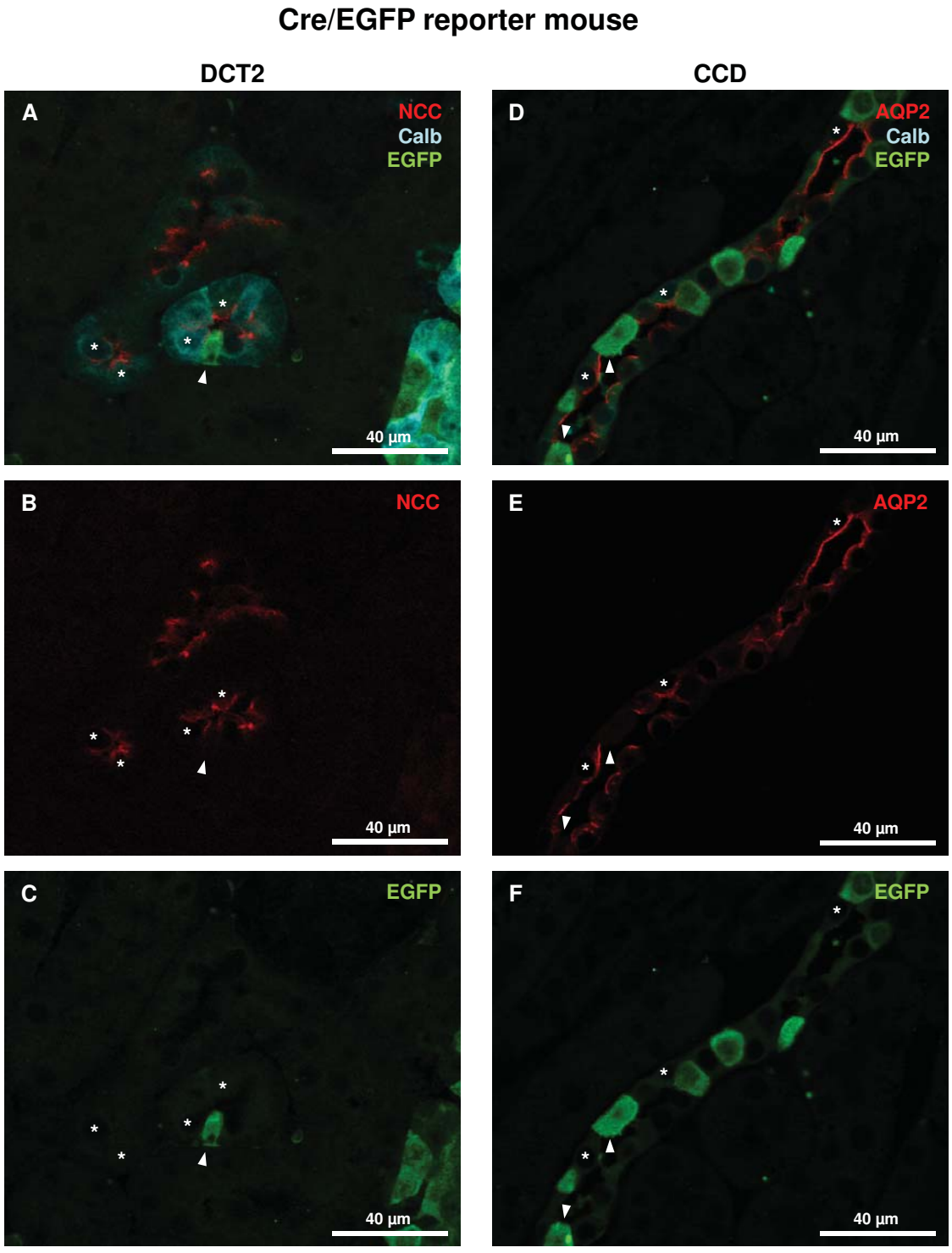
Cre/EGFP reporter mouse
DCT2
CCD
A
NCC
Calb
EGFP
40 µm
D
AQP2
Calb
EGFP
40 µm
B
NCC
40 µm
E
AQP2
40 µm
C
EGFP
40 µm
F
EGFP
40 µm

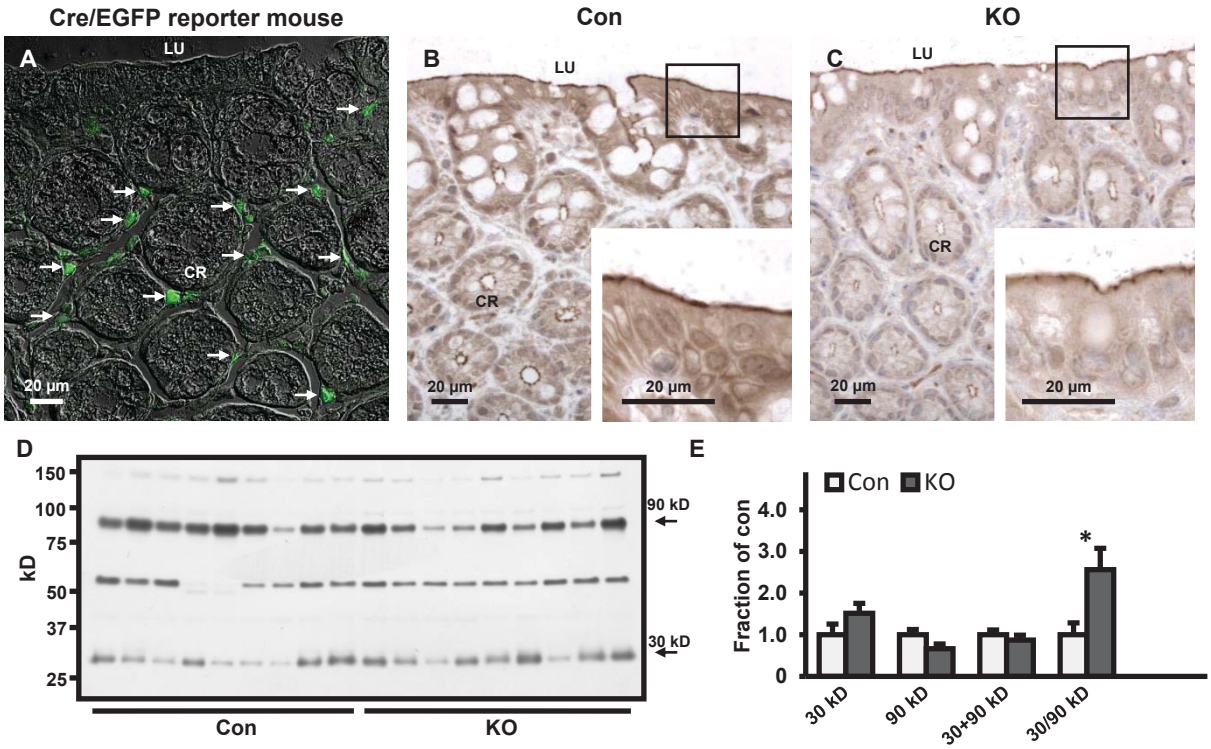
Cre/EGFP reporter mouse
Con
KO
A
LU
CR
20 μm
B
LU
CR
20 μm
20 μm
C
LU
CR
20 μm
20 μm
D
150
100
75
50
37
25
kD
90 kD
30 kD
Con
KO
E
Con
KO
Fraction of con
4.0
3.0
2.0
1.0
0
*
30 kD
90 kD
30+90 kD
30/90 kD

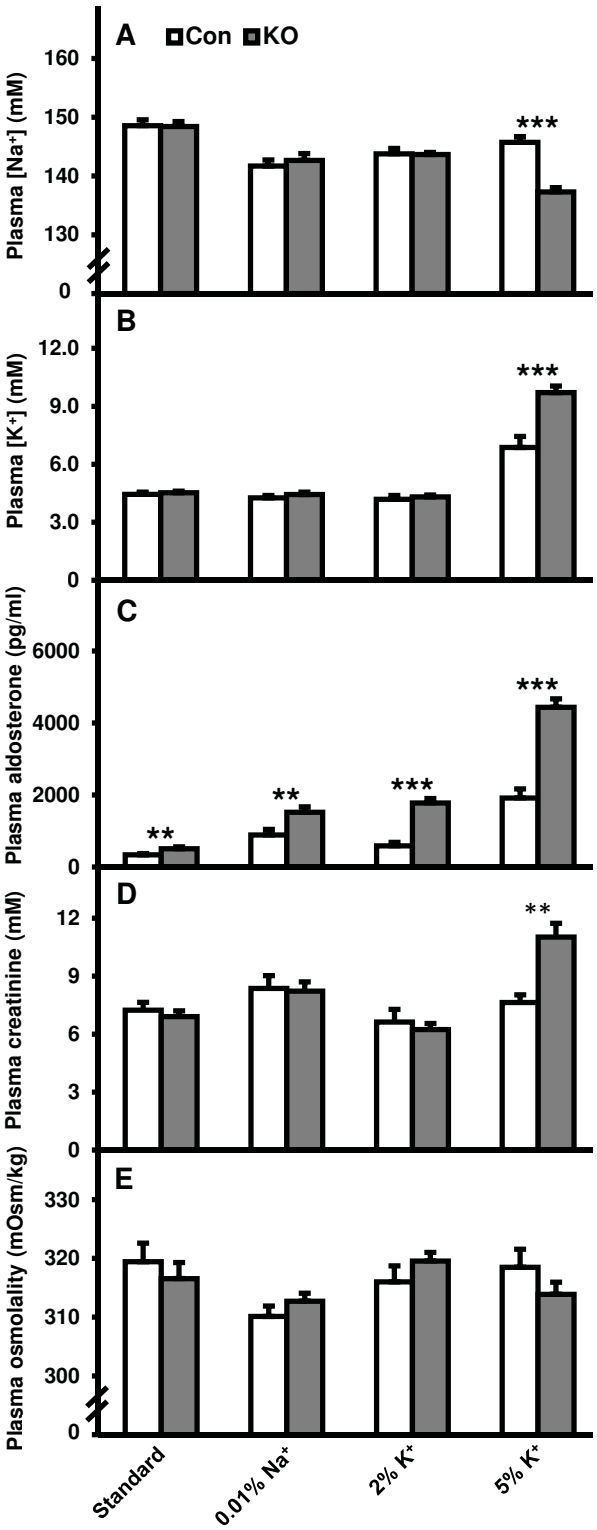
A
Con
KO
Plasma [Na+] (mM)
160
150
140
130
0
***
B
Plasma [K+] (mM)
12.0
9.0
6.0
3.0
0
***
C
Plasma aldosterone (pg/ml)
6000
4000
2000
0
**
**
***
***
D
Plasma creatinine (mM)
12
9
6
3
0
**
E
Plasma osmolality (mOsm/kg)
330
320
310
300
0
Standard
0.01% Na+
2% K+
5% K+

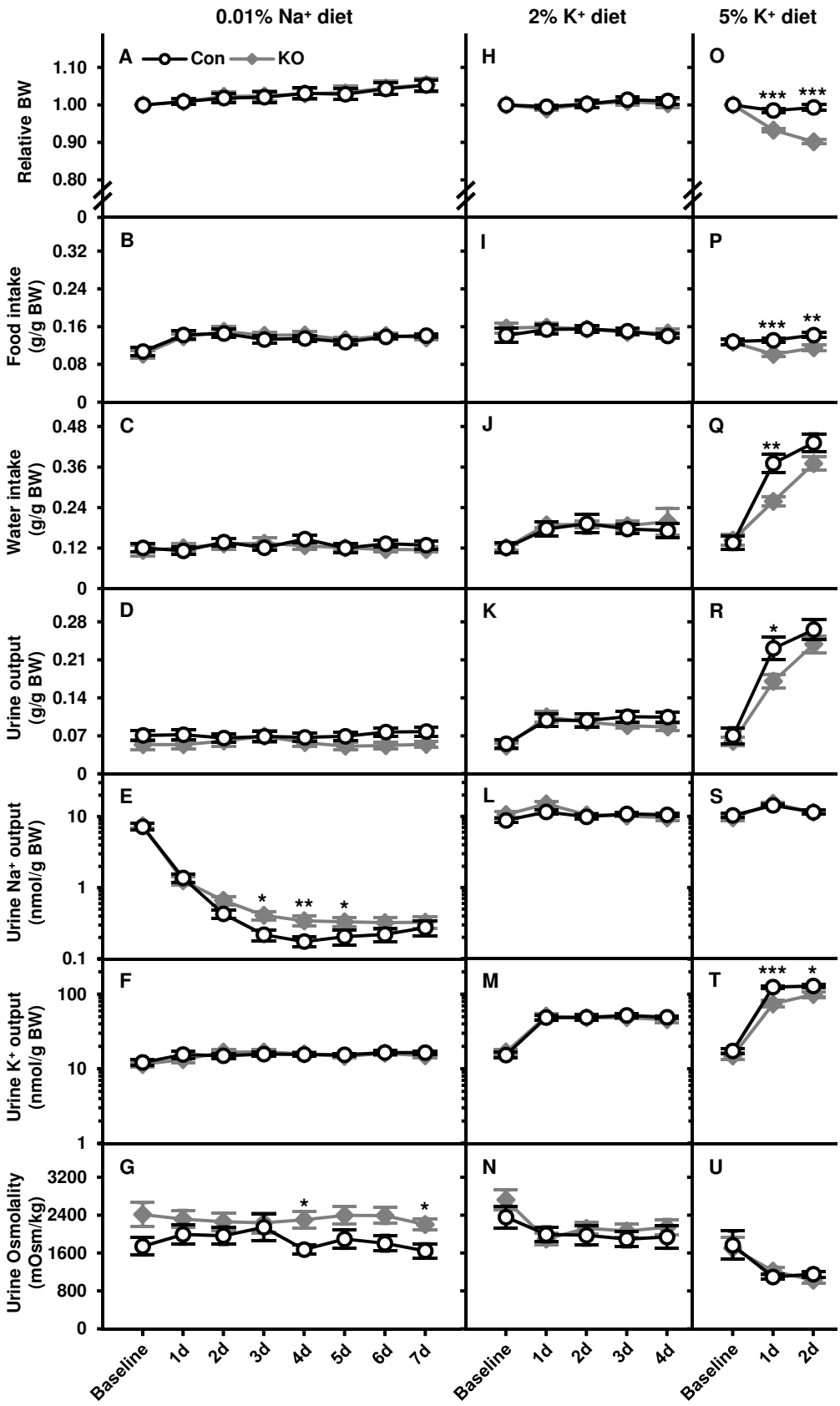
0.01% Na+ diet
2% K+ diet
5% K+ diet
A
Con
KO
H
O
Relative BW
1.10
1.00
0.90
0.80
0
***
***
B
I
P
Food intake (g/g BW)
0.32
0.24
0.16
0.08
0
***
**
C
J
Q
Water intake (g/g BW)
0.48
0.36
0.24
0.12
0
**
D
K
R
Urine output (g/g BW)
0.28
0.21
0.14
0.07
0
*
E
L
S
Urine Na+ output (nmol/g BW)
10
1
0.1
*
**
*
F
M
T
Urine K+ output (nmol/g BW)
100
10
1
***
*
G
N
U
Urine Osmolality (mOsm/kg)
3200
2400
1600
800
0
*
*
Baseline
1d
2d
3d
4d
5d
6d
7d
Baseline
1d
2d
3d
4d
Baseline
1d
2d

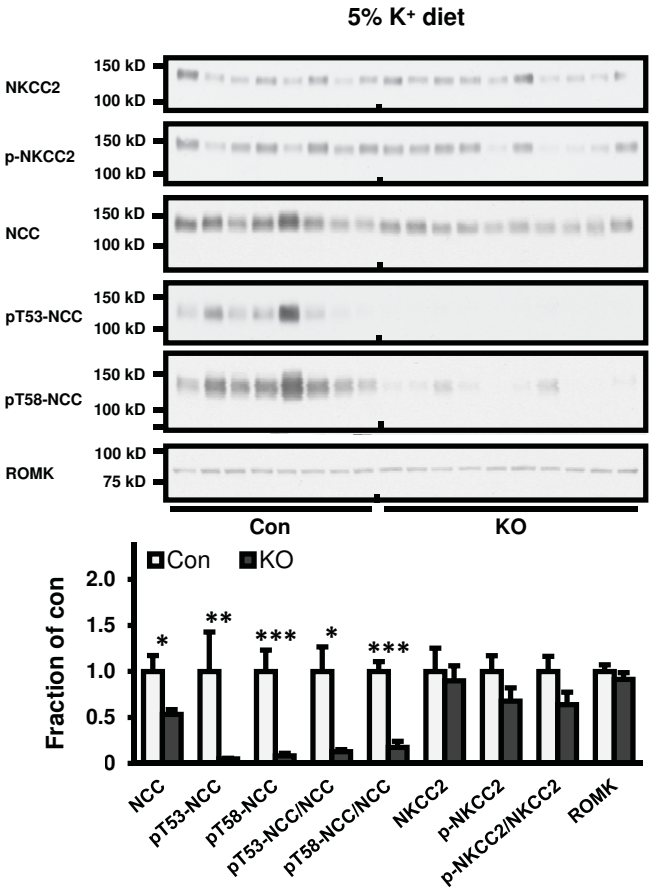
5% K+ diet
NKCC2
150 kD
100 kD
p-NKCC2
150 kD
100 kD
NCC
150 kD
100 kD
pT53-NCC
150 kD
100 kD
pT58-NCC
150 kD
100 kD
ROMK
100 kD
75 kD
Con
KO
Con
KO
Fraction of con
2.0
1.5
1.0
0.5
0
*
**
***
*
***
NCC
pT53-NCC
pT58-NCC
pT53-NCC/NCC
pT58-NCC/NCC
NKCC2
p-NKCC2
p-NKCC2/NKCC2
ROMK